

## Research Article

# Fabrication of Carbamazepine Cocrystals: Characterization, *In Vitro* and Comparative *In Vivo* Evaluation

Muhammad Wasim,<sup>1</sup> Abdul Mannan,<sup>1</sup> Muhammad Hassham Hassan Bin Asad <sup>1,2</sup>,  
Muhammad Imran Amirzada,<sup>1</sup> Muhammad Shafique,<sup>3</sup> and Izhar Hussain <sup>1</sup>

<sup>1</sup>Department of Pharmacy, COMSATS University Islamabad, Abbottabad Campus Abbottabad 22060, Pakistan

<sup>2</sup>Institute of Fundamental Medicine and Biology, Department of Genetics, Kazan Federal University, Kazan 420008, Russia

<sup>3</sup>Department of Pharmaceutical Science, College of Pharmacy-Boys, Shaqra University, Al-Dawadmi Campus 17441, Shaqra 11911, Saudi Arabia

Correspondence should be addressed to Muhammad Hassham Hassan Bin Asad; hasshamasad@yahoo.com and Izhar Hussain; izharhussain@cuiatd.edu.pk

Received 3 November 2020; Revised 25 January 2021; Accepted 5 March 2021; Published 16 March 2021

Academic Editor: Dr. Abdul Ahad

Copyright © 2021 Muhammad Wasim et al. This is an open access article distributed under the Creative Commons Attribution License, which permits unrestricted use, distribution, and reproduction in any medium, provided the original work is properly cited.

Carbamazepine (CBZ) is an antiepileptic drug having low bioavailability due to its hydrophobic nature. In the current study, efforts are made to investigate the effect of dicarboxylic acid coformer spacer groups (aliphatic chain length) on physicochemical properties, relative humidity (RH) stability, and oral bioavailability of CBZ cocrystals. Slurry crystallization technique was employed for the preparation of CBZ cocrystals with the following coformers: adipic (AA), glutaric (GA), succinic (SA), and malonic acid (MA). Powder X-ray diffractometry and Fourier-transform infrared spectroscopy confirmed cocrystal preparation. Physicochemical properties, RH stability, and oral bioavailability of cocrystals were investigated. Among the prepared cocrystals, CBZ-GA showed maximum solubility as well as improved dissolution profile (CBZ-GA > CBZ-MA > CBZ-AA > pure CBZ > CBZ-SA) in ethanol. Maximum RH stability was shown by CBZ-AA, CBZ-SA, and CBZ-MA. *In vivo* studies confirmed boosted oral bioavailability of cocrystals compared to pure CBZ. Furthermore, *in vivo* studies depicted the oral bioavailability order of cocrystals as CBZ-GA > CBZ-MA > Tegral® > CBZ-AA > CBZ-SA > pure CBZ. Thus, pharmaceutical scientists can effectively employ cocrystallization technique for tuning physicochemical properties of hydrophobic drugs to achieve the desired oral bioavailability. Overall, results reflect no consistent effect of spacer group on physicochemical properties, RH stability, and oral bioavailability of cocrystals.

## 1. Introduction

Pharmaceutical cocrystal (multicomponent system) consists of an active pharmaceutical ingredient (API) and coformer/co-crystal former [1]. The combination of chemically different components in a precise stoichiometric ratio leads to the formation of cocrystal [2]. The noncovalent interactions like *pi-pi* interactions, Van der Waals forces, and hydrogen bonding are predominantly present between the molecules of crystalline complex [3, 4]. Pharmaceutical cocrystallization is a good technique for enhancing the physicochemical properties of active pharmaceutical ingredients [5]. Physicochemical properties include solubility, dissolution, melting point, bulk

density, hygroscopicity, and compressibility [1–3, 6]. Dissolution and solubility have primary significance owing to their principal role in drug oral absorption [7]. Many cocrystals have been synthesized for modification of physicochemical properties like posaconazole–4-aminobenzoic acid which exhibited high solubility and improved dissolution [8]. Similarly, improved dissolution rate and aqueous solubility were observed by carbamazepine–cinnamic acid cocrystal compared to pure carbamazepine (CBZ) [9]. Cocrystal temozolomide with baicalein enhanced oral drug bioavailability [10]. Carbamazepine–succinic acid cocrystal showed improved physicochemical properties and oral bioavailability [11]. Solubility, dissolution, and stability are the actual significant part of

the cocrystal studies. Two factors determined the solubility: cocrystal components solvation and crystal lattice energy. Both factors can be influenced to various extents by cocrystallization [12, 13]. Over the last decade, different studies have been performed on many CBZ (BCS class II) cocrystals to increase its solubility. The low bioavailability of CBZ is due to poor solubility [14]. As stated by biopharmaceutical classification system (BCS), drugs having low solubility despite of high permeability are considered BCS class II drugs. These drugs have dissolution-restricted absorption and low oral bioavailability [15]. Therefore, to get the desired therapeutic effect, CBZ is used generally in a high dose [14].

Many cocrystals have been reported with a series of dicarboxylic acid cofomers, for instance, itraconazole cocrystals with cofomers like pimelic, adipic, glutaric, succinic, malonic, and oxalic acid; pyrazinecarboxamide with glutaric, succinic, and malonic acid cofomers [13]; and CBZ cocrystals with malonic, succinic, glutaric, and adipic acid [16–18]. Different stoichiometry of CBZ cocrystal with cofomers malonic (1:1; 2:1), succinic (2:1), adipic (2:1), and glutaric acid (1:1) has been reported [19]. Pyrazine was cocrystallized with a varying aliphatic chain length (spacer group) of dicarboxylic acid cofomers to determine the influence on cocrystal formation and resulting structure of cocrystals [20]. If the spacer group of cofomer changes, the conformation as well as the structure of crystal changes. Hence, self-assemblies formation by carboxylic acid cofomers having flexible aliphatic spacer group cause changes in alignment and geometries of donors and acceptors [21]. Therefore, it is important to understand the influence of spacer group in dicarboxylic acid cofomers (COOH)-(CH<sub>2</sub>)<sub>n</sub>-(COOH) (Figure 1): malonic (MA, *n* = 1), succinic (SA, *n* = 2), glutaric (GA, *n* = 3), and adipic acid (AA, *n* = 4) on physicochemical properties and oral bioavailability of CBZ cocrystals.

## 2. Materials and Methods

**2.1. Materials.** CBZ was obtained from Tokyo Chemical Industry, Europe. The dicarboxylic acid cofomers, MA, SA, and AA, were purchased from Acros Organics, while GA was procured from Sigma-Aldrich. All analytical grade solvents were purchased from commercial sources.

**2.2. Cocrystal Preparation.** Slurry crystallization method was used for bulk production of each cocrystal in different solvents. Solvents were added in screw-capped glass vials having solid, without reaching full dissolution. The mixtures were stirred for 72 hours at room temperature using a magnetic stirring bar. For further characterization, the resulting powder was rapidly filtered and dried. The detail is given in Table 1.

### 2.3. Characterization

**2.3.1. Powder X-Ray Diffractometry.** Samples were characterized employing the XRPD method on a diffractometer (Siemens D5000). Samples were irradiated using Cu as the X-ray source at a current and voltage of 40 mA and 40 kV, respectively. A secondary monochromator was used to allow selection of the K $\alpha$  radiation of Cu ( $\lambda = 1.5418 \text{ \AA}$ ). The

samples were measured with a continuous scan rate of 0.01°/s from 2 to 50° at 2 $\theta$ .

**2.3.2. Fourier-Transform Infrared Spectroscopy.** An approximately 3–7 mg of samples was placed on crystal surface (diamond) to obtain the FT-IR spectra by using the PerkinElmer FT-IR spectrophotometer. The FT-IR spectral analysis of finely pulverized samples were carried out at a wavelength range of 450–4000 cm<sup>-1</sup>.

**2.4. In Vitro Studies.** *In vitro* studies like solubility and dissolution were performed for the prepared samples. Concerning dissolution experiments, the initial step was to grind CBZ cocrystals in mortar and pestle to obtain uniform particle size range. In the next step, the instrument (EasyMax 102 Advanced Synthesis Workstation) devised by Mettler Toledo provided with a temperature monitor and a stirrer rotating at 150 rpm to prepare supersaturated CBZ solution by pouring large quantity of sample powder in a flask (100 mL) having a medium (ethanol) of 40 mL at 25°C. Online “React IR iC 10” manufactured by Mettler Toledo AutoChem having an ATR crystal (AgX DiComp Fiber Conduit probe) with a size 6.5 mm attached to the crystallization reactor was used for recording of CBZ IR signature in solution every 15 seconds (50 scans) from 2800 cm<sup>-1</sup> to 650 cm<sup>-1</sup> till equilibrium. Finally, the React IR data was monitored using the “IR iC 10” software. The samples for solubility measurement were collected when the cocrystal solution reached the saturated state during dissolution experiment. Samples were analyzed by high-performance liquid chromatography (HPLC).

**2.5. Relative Humidity Stability Study.** Different relative humidity (RH) conditions like 43%, 75%, and 98% were obtained using salt solutions (saturated) of KCO<sub>3</sub>, NaCl, and K<sub>2</sub>SO<sub>4</sub>, respectively. The samples were kept in three different RH conditions for a period of 1 month. The samples were then immediately analyzed for absorption/adsorption of water by TGA-SDTA 851e devised by the Mettler Toledo thermogravimetric analysis (TGA) technique. The TGA thermograms were recorded at a temperature range of 30–150°C with a scanning rate of 10°C/min under a nitrogen purge of 50 mL min<sup>-1</sup>. The solid samples of masses around 8–10 mg were analyzed using aluminum oxide crucible. The STARe thermal analysis software was used for data evaluation.

**2.6. Filling of Capsule Shells.** Though capsule filling is a technical process, for research purposes, filling of capsules does not require specific machines due to small batch size. Therefore, all the suitable size capsules for *in vivo* pharmacokinetic studies were filled manually.

### 2.7. In Vivo Pharmacokinetic Studies

**2.7.1. Animals and Dosing.** The protocols used for *in vivo* pharmacokinetic studies with the approval of “Research Ethical Committee” Department of Pharmacy, COMSATS University Islamabad (CUI), Abbottabad Campus (ref. no PHM-0088/E.C/M5). Healthy rabbits with a body weight 2 ± 0.3 kg were housed and restrained from food about 12 hours prior dosing while being allowed free access to water.

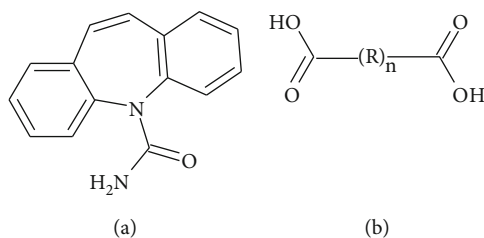


FIGURE 1: Chemical structures of (a) carbamazepine and (b) coformers (R-spacer group,  $n = 1, 2 \dots$ ).

TABLE 1: Complete detail about cocrystals regarding their preparation.

API	Coformer	Ratio	Solvent	Stirring time (h)
CBZ	AA	2 : 1	Methanol	72
CBZ	GA	1 : 1	Acetone	72
CBZ	SA	2 : 1	Ethanol	72
CBZ	MA	2 : 1	Methanol	72

Abbreviations: CBZ: carbamazepine, MA: malonic acid, SA: succinic acid, GA: glutaric acid, AA: adipic acid.

All rabbits were randomly divided into five groups, each having six rabbits. Cocrystals and commercial product (pulverized) were filled into capsules and orally administered with 2 mL of water. Blood samples (0.5 mL) at different time intervals (0 to 18 h) were collected in heparinized tubes followed by separation of plasma by centrifugation for 10 min at 12000 rpm and then stored until further analysis at  $-20^{\circ}\text{C}$ .

**2.7.2. Quantification of CBZ Plasma Concentration.** CBZ was quantified in plasma samples as described previously [22] with slight modification, using the HPLC (series 200, PerkinElmer USA) technique. Mobile phase of acetonitrile, methanol, and phosphoric acid buffer (pH 6.5) 0.1 mol/L at a ratio of 10:30:60 was used. The flow rate and retention time were 1.2 mL/min and 3.2 min, respectively. A  $250 \times 4.6$  mm Supelco<sup>®</sup> C<sub>18</sub> ( $5 \mu\text{m}$  particle size) was used as an analytical column. Acetonitrile was added to samples and centrifuged to precipitate proteins. A  $20 \mu\text{L}$  supernatant was injected. CBZ concentration was measured at  $\lambda_{\text{max}}$  285 nm by UV detector.

**2.7.3. Data Analysis.** Pharmacokinetic (PK) parameters like peak plasma concentration ( $C_{\text{max}}$ ) and time to reach peak plasma concentration ( $T_{\text{max}}$ ) were measured for noncompartmental model. Trapezoidal rule was employed for the calculation of area under curve ( $\text{AUC}_{0 \rightarrow t}$ ) from the concentration–time curve. Equation (1) was used for the calculation of total area under the curve ( $\text{AUC}_{0 \rightarrow 18}$ ):

$$\text{AUC}_{0 \rightarrow 18} = \text{AUC}_{0 \rightarrow 18} + \frac{C_t}{K_e}, \quad (1)$$

where  $K_e$  is CBZ elimination rate constant (apparent),  $C_t$  is CBZ concentration at 18th hour, and ANOVA (one-way analysis of variance) and  $t$ -test ( $p < 0.05$ ) were used for comparison of PK parameters and statistical analysis of data.

### 3. Results

The powder XRPD patterns of cocrystals are different from their individual components, i.e., CBZ and respective coformers. The XRPD patterns of CBZ-AA, CBZ-GA, CBZ-SA, and CBZ-MA are perfectly matched with their XRPD powder patterns provided in the Cambridge Structural Database (CSD) as MOXVEB, MOXVOL, XOBCEB, and XOBCEX, respectively (Figure 2). FT-IR spectra of cocrystals are different from their individual components, i.e., pure CBZ and respective coformers as shown in Figure 3. *In vitro* studies, like solubility and dissolution behavior of pure CBZ and its four cocrystals, were investigated. The dissolution of cocrystals was improved except CBZ-SA compared to pure CBZ as shown in Figure 4. Cocrystals showed better dissolution whose solubility was enhanced by cocrystallization. The result is summarized in Table 2. The results of RH stability studies of pure CBZ show a weight loss of 10.7% and 1.9% at 98% and 75% RH conditions, respectively. CBZ-AA and CBZ-SA showed maximum stability with no weight loss. CBZ-GA, the most unstable, even showed a weight loss at 43% RH as shown in Figure 5 and Table 3. A probe into the *in vivo* pharmacokinetic study was conducted in rabbits. Plasma drug profile of pure CBZ, cocrystals, and marketed product is shown in Figure 6. Significant increase in oral bioavailability was observed with cocrystals compare to pure CBZ. CBZ-GA exhibited the highest peak plasma concentration ( $7 \pm 0.35 \mu\text{g/mL}$ ) with high oral bioavailability ( $64 \pm 2.2 \mu\text{g h/mL}$ ). Table 4 enlists pharmacokinetic parameters.

### 4. Discussion

The characteristic XRPD peaks of polymorph CBZ-III<sup>#</sup> (Figure S1), used in the study that appeared at  $2\theta = 15.8$  and  $18.6$ , were found to be in good agreement with reported data [23]. CBZ was cocrystallized with dicarboxylic acid coformers, i.e., AA, GA, SA, and MA to investigate the spacer group effects on physicochemical properties and oral bioavailability of cocrystals. The formation of cocrystals was confirmed by XRPD and FT-IR. The XRPD pattern of samples was in good agreement with their corresponding XRPD patterns in CSD. Figure 2 shows overlays of XRPD pattern of cocrystals consistent with the published data [24]. There are two reported polymorphs of CBZ-MA cocrystals with CSD codes XOBCEB (2:1) and MOXVUR (1:1) as shown in Figure S1 [19]; a third form has also been studied, but a single crystal was not yet obtained via solvent crystallization method [25]. CBZ-MA and CBZ-SA have similar packing of CBZ and hydrogen-bonding motif. So these two are isostructural [19].

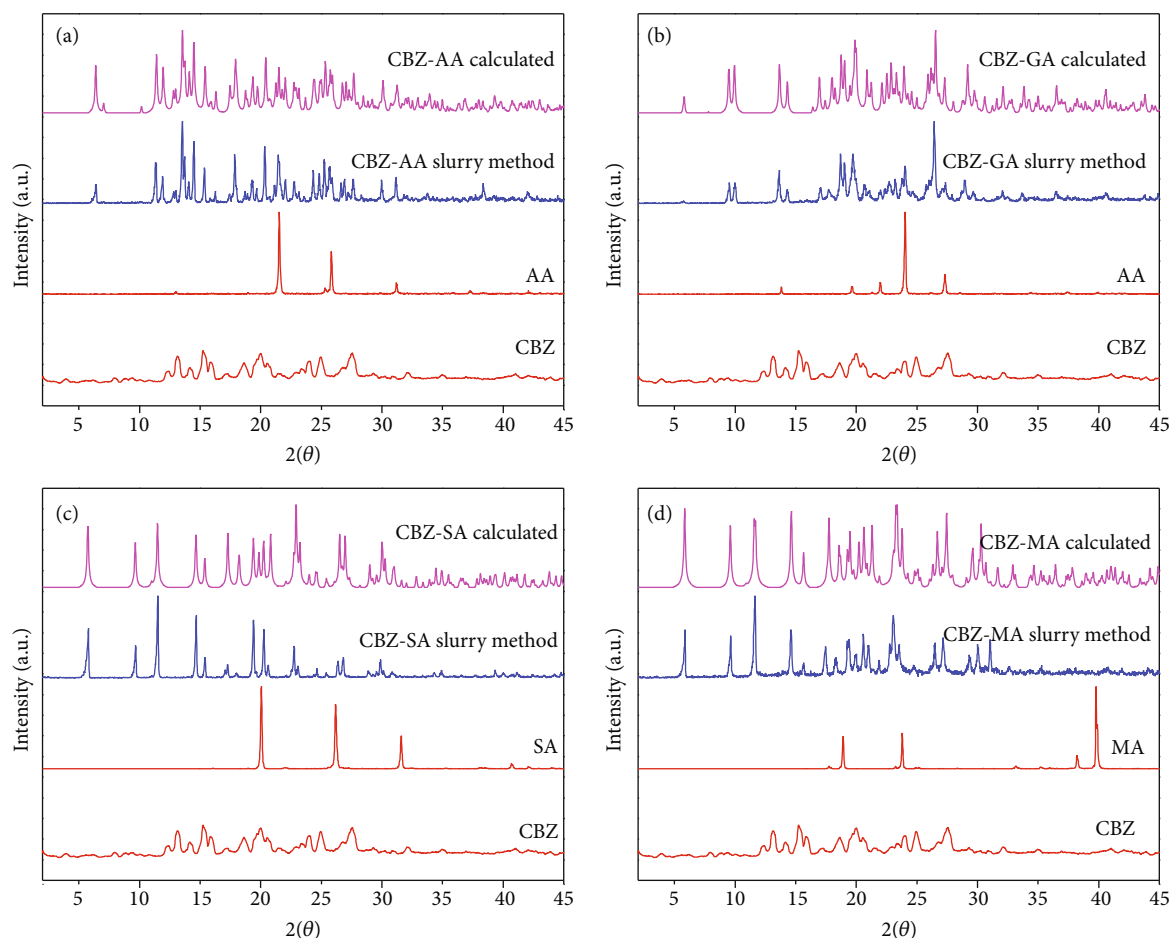


FIGURE 2: XRPD patterns of (a) CBZ-AA, (b) CBZ-GA, (c) CBZ-SA, and (d) CBZ-MA cocrystals.

Further validation of cocrystals was carried out by FT-IR spectral analysis. The FT-IR spectra of cocrystals are different from their respective components (Figure 3 and Table 5). The pure CBZ shows the absorption bands of N-H stretching and C=O stretching at  $3465$  and  $1675\text{ cm}^{-1}$ , respectively [26]. Clear shifts were observed in CBZ-AA, CBZ-GA, CBZ-SA, and CBZ-MA cocrystals due to hydrogen-bond formation. Thus, the XRPD and FT-IR analyses authenticate the formation of CBZ cocrystals with AA, GA, SA, and MA cofomers.

*In vitro* results of CBZ cocrystals showed that about 60% of pure CBZ was dissolved in 45 min. But CBZ-SA cocrystal dissolved 52% in 45 min being the lowest soluble, whereas dissolution of CBZ-GA, CBZ-MA, and CBZ-AA was 97%, 90%, and 70%, respectively (Figure 4). CBZ-GA (1:1) showed highest solubility ( $24.92 \pm 0.03\text{ mg/mL}$ ), while CBZ-SA (2:1) cocrystal exhibited low solubility of  $8.88 \pm 0.01\text{ mg/mL}$  as shown in Table 2. Thus, the CBZ to cofomer stoichiometry seems to have no effect on solubility as well as dissolution. The higher final concentration of CBZ was achieved by all cocrystals except CBZ-SA compared to pure CBZ. This might be due to CBZ-SA cocrystal being low soluble in ethanol [27]. The interesting thing is that maximum solubility of CBZ was observed in 40 minutes by all cocrys-

tals, whereas approximately 100-minute longer time was needed for pure CBZ. In cocrystal, the more soluble component (coformer) is usually drawn out of the crystal lattice into dissolution medium [28]. The solubility of dicarboxylic acids series in different solvents including ethanol was determined by Zhang and coworkers to check the effect of “even-odd” number of carbons. The solubility of cofomer having odd number of carbons was higher compared to cofomer of even number of carbons [29]. Thus, the “even-odd” number of carbons of cofomers may also affect the solubility of cocrystal. In our study results, it has been noted that cocrystals having cofomer (odd number of carbons) showed higher solubility and vice versa (Table 2). Likewise, in the previous study, the solubility order of cofomers (GA > MA > AA > CBZ-SA) in ethanol has been reported [29]. Our results of cocrystal solubility are consistent with the order of solubility of cofomers. From a pharmaceutical point of view, a significant dissolution profile was observed by CBZ-GA being the most soluble released about 97% CBZ in dissolution medium. The enhanced solubility and dissolution of CBZ-GA in the presence of excess cofomer is also reported [30]. Past studies also explored that dissolution and solubility can be improved by cocrystallization technique [8, 31–33]. Likewise, an improved dissolution rate by carbamazepine–cinnamic acid

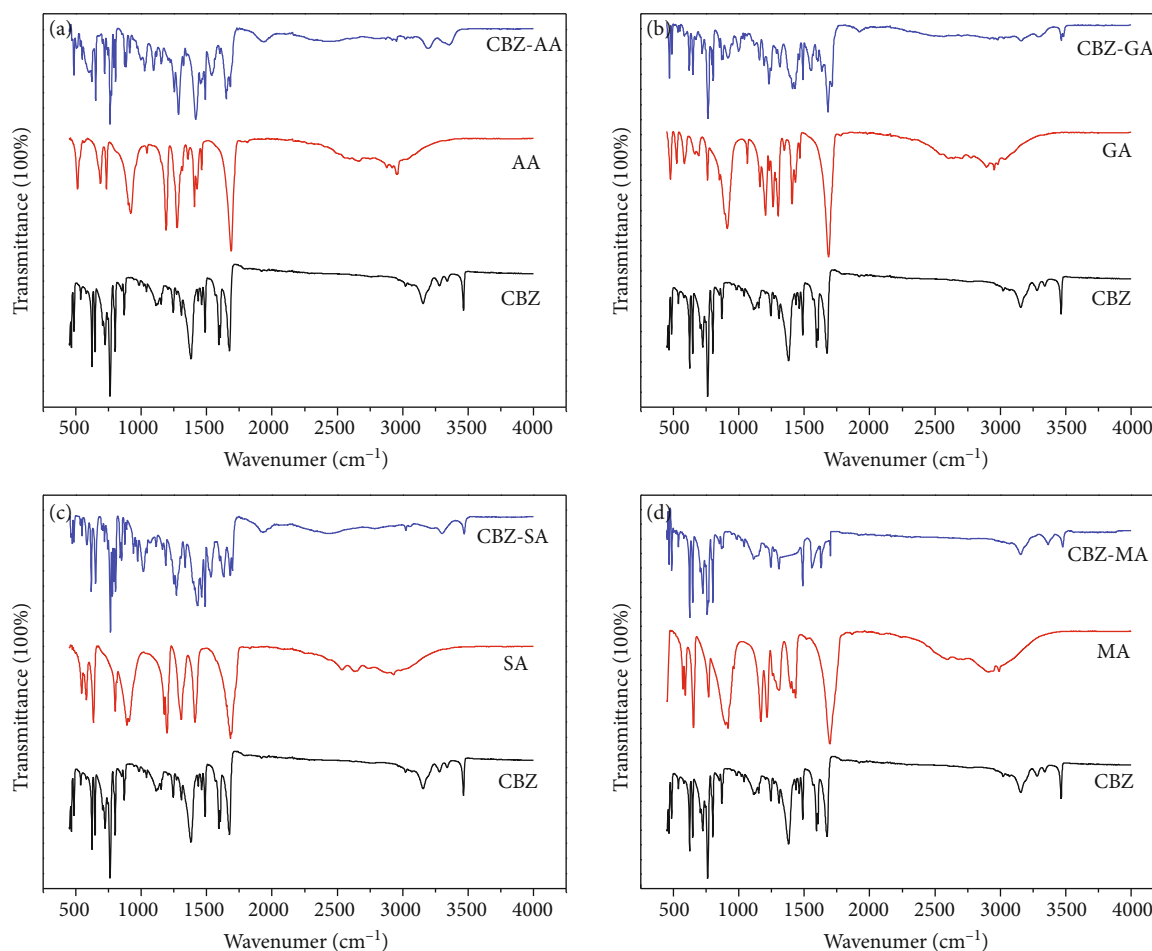


FIGURE 3: FT-IR spectra of (a) CBZ-AA, (b) CBZ-GA, (c) CBZ-SA, and (d) CBZ-MA cocrystals.

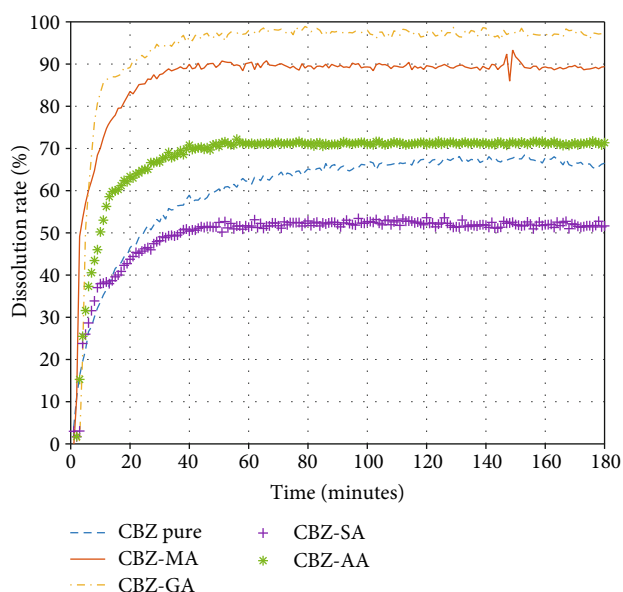


FIGURE 4: Dissolution release profile of CBZ-AA, CBZ-GA, CBZ-SA, CBZ-MA, and pure CBZ in ethanol.

TABLE 2: Solubility and % dissolution rate about different cocrystals in ethanol.

S. No.	Samples	Cocrystal stoichiometry	Solubility (mg/mL)	% dissolution rate (45 min)
01	CBZ	—	18.19 ± 0.06	60
02	CBZ-MA	2 : 1	24.61 ± 0.08	90
03	CBZ-SA	2 : 1	8.88 ± 0.01	52
04	CBZ-GA	1 : 1	24.92 ± 0.03	97
05	CBZ-AA	2 : 1	22.62 ± 0.10	70

cocrystal was observed in distilled water compared to pure CBZ [9]. Therefore, enhanced dissolution of cocrystals can be attributed to solubility improvement in the dissolution medium.

Concerning RH stability studies, CBZ-GA showed % weight loss of 0.7, 2.1, and 6 at 43, 75, and 98% RH conditions, respectively, whereas CBZ-SA and CBZ-AA showed zero % weight loss at provided RH conditions. The weight loss of 11.7% was observed in CBZ-MA at 98% RH and remained stable at 43 and 75% RH. However, the trend of % weight loss in pure CBZ was 1.9 and 10.7 at 75% and

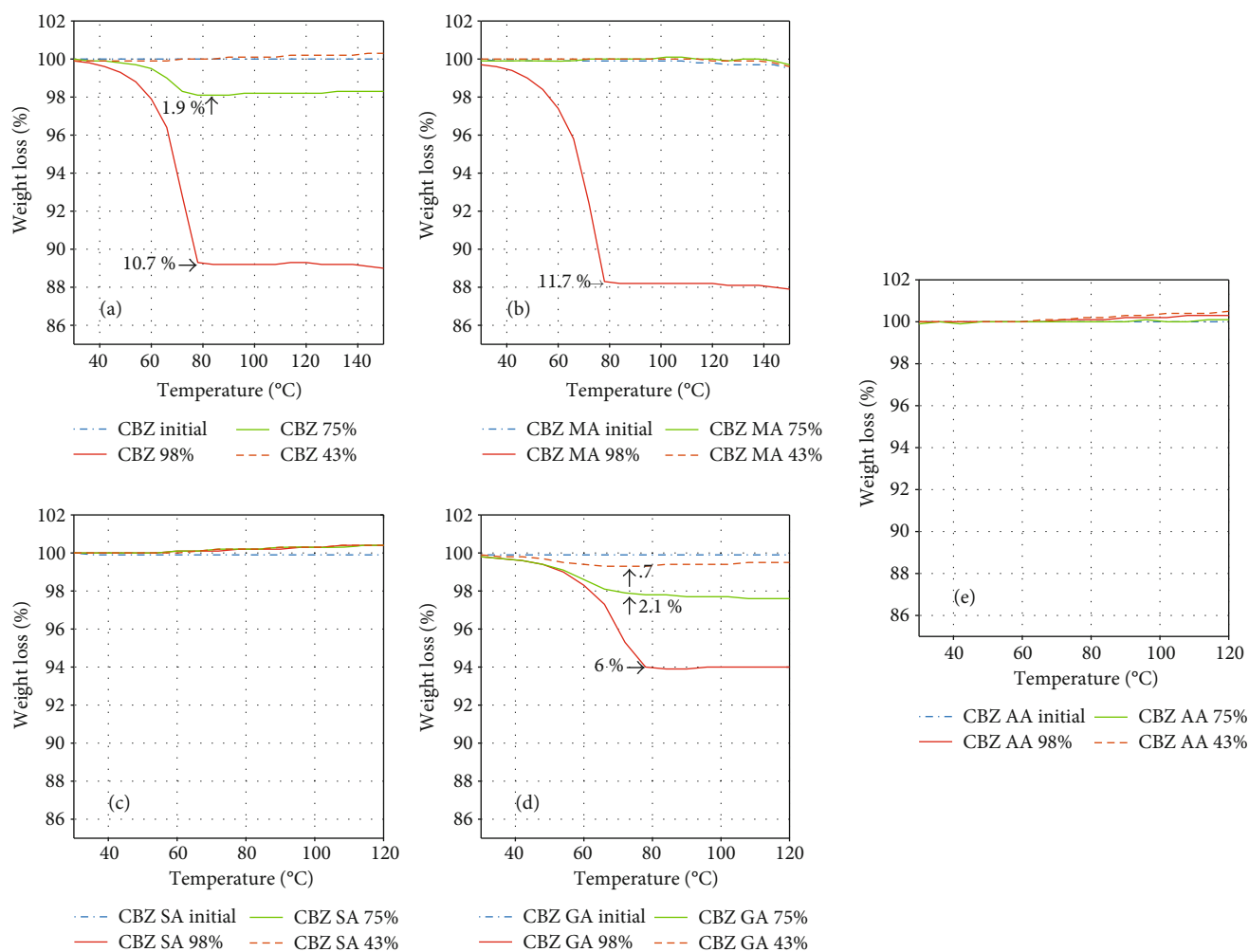


FIGURE 5: TGA thermograms of (i) pure CBZ, (ii) CBZ-MA, (iii) CBZ-SA, (iv) CBZ-GA, and (v) CBZ-AA.

TABLE 3: The % weight loss of pure CBZ, CBZ-MA, CBZ-SA, CBZ-GA, and CBZ-AA.

Samples	% relative humidity	% weight loss
CBZ	43	—
	75	1.9
	98	10.7
CBZ-MA	43	—
	75	—
	98	11.7
CBZ-SA	43	—
	75	—
	98	—
CBZ-GA	43	0.7
	75	2.1
	98	6
CBZ-AA	43	—
	75	—
	98	—

98% RH, respectively, while stable at 43% RH condition as shown in Figure 5 and Table 3. So, overall, CBZ-RH stability has been improved by cocrystallization. It was observed that CBZ-GA is the most unstable cocrystal with highest solubility and improved dissolution. It was also seen in the previous studies that a highly soluble cocrystal is least stable [34]. A pure CBZ and cocrystals were evaluated for oral bioavailability in rabbits along with marketed product to assess the spacer group effect and to confirm the *in vitro* improvement of CBZ cocrystals translation into *in vivo* pharmacokinetic benefit. The plasma drug concentration vs. time profile and pharmacokinetic parameters are given in Figure 6 and Table 4, respectively. The results of *in vivo* pharmacokinetic study showed that highest oral bioavailability ( $64 \pm 2.2 \mu\text{g h/mL}$ ) and  $C_{\text{max}}$  ( $7 \pm 0.35 \mu\text{g/mL}$ ) were observed by CBZ-GA. The oral bioavailability of CBZ-GA was significantly higher than pure CBZ ( $29.87 \pm 2.1 \mu\text{g h/mL}$ ) and marketed product ( $56.03 \pm 1.2 \mu\text{g h/mL}$ ). The  $\text{AUC}_{0-t}$  of CBZ-MA ( $58 \pm 1.8 \mu\text{g h/mL}$ ) was not considerably higher than marketed product. Moreover, the bioavailability and  $C_{\text{max}}$  of prepared cocrystals were much higher than pure CBZ. But, no correlation was observed between oral bioavailability and

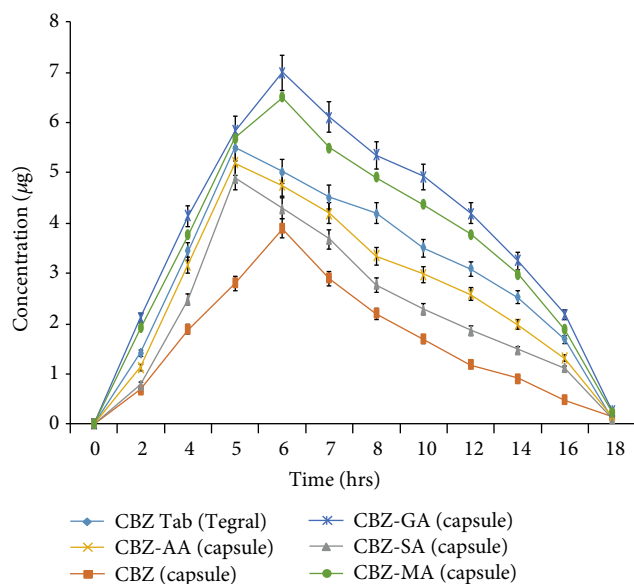


FIGURE 6: *In vivo* drug release profile of pure CBZ, cocrystals, and marketed product.

TABLE 4: Pharmacokinetic parameters of pure CBZ, cocrystals, and marketed product.

Formulation	AUC <sub>0-18</sub> (µg h/mL)	C <sub>max</sub> (µg/mL)	T <sub>max</sub> (h)
CBZ tab (marketed)	56.03 ± 1.2	5.5 ± 0.32	5 ± 0.72
CBZ (capsule)	29.87 ± 2.1	3.9 ± 0.27	6 ± 0.22
CBZ-SA (capsule)	47.81 ± 2.00	4.9 ± 0.31	5 ± 0.23
CBZ-AA (capsule)	50.17 ± 1.00	5.2 ± 0.21	5 ± 0.21
CBZ-GA (capsule)	64 ± 2.2	7 ± 0.35	6 ± 0.27
CBZ-MA (capsule)	58 ± 1.8	6.5 ± 0.30	6 ± 0.38

spacer group of cofomers. However, the *in vivo* study results exhibit that solubility and dissolution-restricted oral bioavailability can be enhanced by the cocrystallization technique.

## 5. Conclusion

The present research work concludes the influence of spacer group (varying aliphatic chain length) on solubility, dissolution, RH stability, and oral bioavailability of CBZ cocrystals with dicarboxylic acids cofomers. According to the reported results, a good improvement in dissolution is shown by CBZ-GA being the most soluble and unstable cocrystal. The low soluble cocrystal is CBZ-SA which does not show improved dissolution. Hence, the order of enhanced solubility and dissolution is CBZ-GA ( $n = 3$ ) > CBZ-MA ( $n = 1$ ) > CBZ-AA ( $n = 4$ ) > pure CBZ > CBZ-SA ( $n = 2$ ). The highly and poorly soluble cocrystals show the highest and lowest dissolution, respectively. So, solubility and dissolution are consistent with each other. Similarly, the increased order of oral bioavailability observed is CBZ-GA ( $n = 3$ ) > CBZ-MA ( $n = 4$ ) > mar-

TABLE 5: FT-IR peaks summary of individual components and respective cocrystals.

Compounds	Peaks (cm <sup>-1</sup> )	Groups	Inference
CBZ	3465	N-H stretching	—
	1675	C=O stretching	
AA	1688	C=O stretching	—
GA	1686	C=O stretching	—
SA	1682	C=O stretching	—
MA	1696	C=O stretching	—
CBZ-AA	3355	N-H stretching	Cocrystal formed
	1698	C=O stretching	
CBZ-GA	3482	N-H stretching	Cocrystal formed
	1712	C=O stretching	
CBZ-SA	3469	N-H stretching	Cocrystal formed
	1698	C=O stretching	
CBZ-MA	3481	N-H stretching	Cocrystal formed
	1701	C=O stretching	

Abbreviations: CBZ: carbamazepine, MA: malonic acid, SA: succinic acid, GA: glutaric acid, AA: adipic acid.

keted product > CBZ-AA ( $n = 2$ ) > CBZ-SA ( $n = 1$ ) > pure CBZ. In conclusion, no consistency of spacer group effects is seen on physicochemical properties (solubility and dissolution) and oral bioavailability of CBZ cocrystals. In other words, increasing hydrophobicity of cofomer has no regular effect on cocrystals physicochemical properties and oral bioavailability.

## Data Availability

Data used to support this study finding have been included in the article and could be provided upon request from first author Muhammad Wasim (wassypharmacist@gmail.com).

## Conflicts of Interest

Authors declare that there is no conflict of interest.

## Acknowledgments

The authors would like to acknowledge the Higher Education Commission (HEC), Pakistan, for supporting the six-month research visit to Université Catholique de Louvain, Belgium, under the International Research Support Initiative Program. The authors would also like to gratefully acknowledge the invaluable services and assistance provided by Centralized Resources Laboratory (CRL), Peshawar University for *in vivo* pharmacokinetic study. Moreover, authors highly acknowledge Dr. Muhammad Hassham Hassan Bin Asad (KFU, Russia; CUI, Pakistan) for his valuable support to publish this research work.

## Supplementary Materials

Figure S1: it contains XRPD patterns of different forms of CBZ and CBZ-MA. (*Supplementary Materials*)

## References

- [1] D. D. Gadade and S. S. Pekamwar, "Pharmaceutical cocrystals: regulatory and strategic aspects, design and development," *Advanced pharmaceutical bulletin*, vol. 6, no. 4, pp. 479–494, 2016.
- [2] D. Douroumis, S. A. Ross, and A. Nokhodchi, "Advanced methodologies for cocrystal synthesis," *Advanced Drug Delivery Reviews*, vol. 117, pp. 178–195, 2017.
- [3] M. Chahkandi, M. H. Bhatti, U. Yunus et al., "Novel cocrystal of *N*-phthaloyl- $\beta$ -alanine with 2,2-bipyridyl: Synthesis, computational and free radical scavenging activity studies," *Journal of Molecular Structure*, vol. 1152, pp. 1–10, 2018.
- [4] S. F. Silva Filho, A. C. Pereira, J. M. G. Sarraguça et al., "Synthesis of a glibenclamide cocrystal: full spectroscopic and thermal characterization," *Journal of Pharmaceutical Sciences*, vol. 107, no. 6, pp. 1597–1604, 2018.
- [5] X. Wang, S. Du, R. Zhang, X. Jia, T. Yang, and X. Zhang, "Drug-drug cocrystals: opportunities and challenges," *Asian Journal of Pharmaceutical Sciences*, vol. 2, 2020.
- [6] S. S. A. Abidi, Y. Azim, S. N. Khan, and A. U. Khan, "Sulfaguanidine cocrystals: synthesis, structural characterization and their antibacterial and hemolytic analysis," *Journal of Pharmaceutical and Biomedical Analysis*, vol. 149, pp. 351–357, 2018.
- [7] F. Cao, G. L. Amidon, N. Rodríguez-Hornedo, and G. E. Amidon, "Mechanistic basis of cocrystal dissolution advantage," *Journal of Pharmaceutical Sciences*, vol. 107, no. 1, pp. 380–389, 2018.
- [8] G. Kuminek, K. L. Cavanagh, M. F. M. da Piedade, and N. Rodríguez-Hornedo, "Posaconazole cocrystal with superior solubility and dissolution behavior," *Crystal Growth & Design*, vol. 19, no. 11, pp. 6592–6602, 2019.
- [9] A. Shayanfar, K. Asadpour-Zeynali, and A. Jouyban, "Solubility and dissolution rate of a carbamazepine-cinnamic acid cocrystal," *Journal of Molecular Liquids*, vol. 187, pp. 171–176, 2013.
- [10] J.-M. Li, X.-L. Dai, G.-J. Li, T.-B. Lu, and J.-M. Chen, "Constructing anti-glioma drug combination with optimized properties through cocrystallization," *Crystal Growth & Design*, vol. 18, no. 8, pp. 4270–4274, 2018.
- [11] M. Ullah, I. Hussain, and C. C. Sun, "The development of carbamazepine-succinic acid cocrystal tablet formulations with improved in vitro and in vivo performance," *Drug Development and Industrial Pharmacy*, vol. 42, no. 6, pp. 969–976, 2016.
- [12] N. Rodríguez-Hornedo, S. J. Nehm, K. F. Seefeldt, Y. Pagán-Torres, and C. J. Falkiewicz, "Reaction crystallization of pharmaceutical molecular complexes," *Molecular Pharmaceutics*, vol. 3, no. 3, pp. 362–367, 2006.
- [13] R. Thakuria, A. Delori, W. Jones, M. P. Lipert, L. Roy, and N. Rodríguez-Hornedo, "Pharmaceutical cocrystals and poorly soluble drugs," *International Journal of Pharmaceutics*, vol. 453, no. 1, pp. 101–125, 2013.
- [14] H. Zhang, Y. Zhu, N. Qiao, Y. Chen, and L. Gao, "Preparation and characterization of carbamazepine cocrystal in polymer solution," *Pharmaceutics*, vol. 9, no. 4, 2017.
- [15] E. R. Gaikwad, S. S. Khabade, T. B. Sutar, M. R. Bhat, and S. A. Payghan, "Three-dimensional Hansen solubility parameters as predictors of miscibility in cocrystal formation," *Asian Journal of Pharmaceutics*, vol. 11, no. 4, pp. 302–318, 2017.
- [16] A. Shevchenko, I. Miroshnyk, L.-O. Pietilä et al., "Diversity in itraconazole cocrystals with aliphatic dicarboxylic acids of varying chain length," *Crystal Growth & Design*, vol. 13, no. 11, pp. 4877–4884, 2013.
- [17] Y.-H. Luo and B.-W. Sun, "Pharmaceutical co-crystals of pyrazinecarboxamide (PZA) with various carboxylic acids: crystallography, hirshfeld surfaces, and dissolution study," *Crystal Growth & Design*, vol. 13, no. 5, pp. 2098–2106, 2013.
- [18] K. Moribe, A. Nagai, Y. Hagiwara, W. Limwikrant, K. Higashi, and K. Yamamoto, "Carbamazepine-dicarboxylic acid cocrystal formation induced by multicomponent cogrinding and exchange reaction of dicarboxylic acids," *Journal of the Society of Powder Technology, Japan*, vol. 49, no. 3, pp. 184–190, 2012.
- [19] S. L. Childs, P. A. Wood, N. Rodríguez-Hornedo, L. S. Reddy, and K. I. Hardcastle, "Analysis of 50 crystal structures containing carbamazepine using the materials module of mercury CSD," *Crystal Growth & Design*, vol. 9, no. 4, pp. 1869–1888, 2009.
- [20] G. Dutkiewicz, E. Dutkiewicz, and M. Kubicki, "Even-odd effect in the co-crystals of pyrazine and dicarboxylic acids," *Structural Chemistry*, vol. 26, no. 1, pp. 247–259, 2015.
- [21] B. R. Jali and J. B. Baruah, "Cocrystals of 2,4-diamino-6-phenyl-1,3,5-triazine with dicarboxylic acids," *Journal of Chemical Crystallography*, vol. 43, no. 10, pp. 531–537, 2013.
- [22] A. C. Moffat, M. D. Osselton, and B. Widdop, *Clarke's analysis of drugs and poisons*, vol. 3, no. 4, 2011. Pharmaceutical press London, 2011.
- [23] M. B. Hickey, M. L. Peterson, L. A. Scoppettuolo et al., "Performance comparison of a co-crystal of carbamazepine with marketed product," *European Journal of Pharmaceutics and Biopharmaceutics*, vol. 67, no. 1, pp. 112–119, 2007.
- [24] S. L. Childs, N. Rodríguez-Hornedo, L. S. Reddy et al., "Screening strategies based on solubility and solution composition generate pharmaceutically acceptable cocrystals of carbamazepine," *CrystEngComm*, vol. 10, no. 7, pp. 856–864, 2008.
- [25] W. Limwikrant, A. Nagai, Y. Hagiwara, K. Higashi, K. Yamamoto, and K. Moribe, "Formation mechanism of a new carbamazepine/malonic acid cocrystal polymorph," *International Journal of Pharmaceutics*, vol. 431, no. 1-2, pp. 237–240, 2012.
- [26] Z. Rahman, R. Samy, V. A. Sayeed, and M. A. Khan, "Physico-chemical and mechanical properties of carbamazepine cocrystals with saccharin," *Pharmaceutical Development and Technology*, vol. 17, no. 4, pp. 457–465, 2012.
- [27] N. A. Ramle, S. A. Rahim, N. Anuar, and O. El-Hadad, "Solubility of carbamazepine co-crystals in ethanolic solution," in *Conference Proceedings*, vol. 1879no. 1AIP Publishing LLC.
- [28] D. D. Bavishi and C. H. Borkhataria, "Spring and parachute: how cocrystals enhance solubility," *Progress in Crystal Growth and Characterization of Materials*, vol. 62, no. 3, pp. 1–8, 2016.
- [29] H. Zhang, Q. Yin, Z. Liu et al., "An odd-even effect on solubility of dicarboxylic acids in organic solvents," *The Journal of Chemical Thermodynamics*, vol. 77, pp. 91–97, 2014.
- [30] H. Yamashita and C. C. Sun, "Improving dissolution rate of carbamazepine-glutaric acid cocrystal through solubilization by excess coformer," *Pharmaceutical Research*, vol. 35, no. 1, 2017.
- [31] J. Cadden, W. T. Klooster, S. J. Coles, and S. Aitipamula, "Cocrystals of leflunomide: design, structural, and physico-chemical evaluation," *Crystal Growth & Design*, vol. 19, no. 7, pp. 3923–3933, 2019.
- [32] Y. Huang, G. Kuminek, L. Roy, K. L. Cavanagh, Q. Yin, and N. Rodríguez-Hornedo, "Cocrystal solubility advantage



diagrams as a means to control dissolution, supersaturation, and precipitation,” *Molecular Pharmaceutics*, vol. 16, no. 9, pp. 3887–3895, 2019.

- [33] Y. Gao, H. Zu, and J. Zhang, “Enhanced dissolution and stability of adefovir dipivoxil by cocrystal formation,” *Journal of Pharmacy and Pharmacology*, vol. 63, no. 4, pp. 483–490, 2011.
- [34] D. J. Good and N. Rodríguez-Hornedo, “Solubility advantage of pharmaceutical cocrystals,” *Crystal Growth & Design*, vol. 9, no. 5, pp. 2252–2264, 2009.